Factors Affecting the Durability of Ca-Complexed Methylmethacrylate Copolymer Films Containing $CaO–SiO_2–H_2O$ Macromolecules*

T. SUGAMA, L. E. KUKACKA, N. CARCIELLO, and J. B. WARREN,
Process Sciences Division, Department of Applied Science, Brookhaven National Laboratory, Upton, New York 11973

Synopsis

A $CaO–SiO_2–H_2O$ macromolecular–ionomer complex was found to be formed in the superficial layers of MMA–TMPTMA copolymer composite films made with filler containing hydraulic cement during exposure in an autoclave at temperatures up to 200°C. This complex acted to prevent the hydrothermal deterioration of the original composite films, which is important if the films are used as protective layers on metals. This complex also contributed significantly to hydrophobicity, a low energy surface, and less surface roughness, thereby lowering the intrinsic water permeability of the films. The glass transition temperature T_g and the tensile strength of the complexed films increased with increasing concentration of the cement additive used as a source of Ca^{2+} metallic ions, but they decreased when the cement concentration became excessive because of the chain enlargement caused by the growth of a large quantity of hydrated macromolecules. Ca^{2+} ions were found to migrate from the cement grains in an aqueous medium and to have a crosslinking function connecting the oxidized metal surfaces and the functional carboxylate groups located in the pendent parts of the polymer molecules. The resultant shear bond strength of metal-to-metal lap joint specimens after exposure for 3 days to water at 150°C was twice as high as that for the samples made without cement.

INTRODUCTION

Ca^{2+} ion-complexed poly(methyl methacrylate) (Ca-PMMA) ionomer composites have been studied earlier.[1] The composites contain hydrated calcium–silica ($CaO–SiO_2$) compounds and are formed by ionic reactions between divalent Ca ions released from $CaO–SiO_2$ grains and carboxylate anions (COO^-) yielded during the hydrolysis of functional pendent carboxyl groups in MMA upon exposure to hydrothermally aggressive environments. In the presence of hot water, the hydraulic inorganic $CaO \cdot SiO_2$ grains are progressively converted into highly crystallized macromolecules.[2] These macromolecules are produced in the vicinity of amorphous ionomer chains, and thereby restrict the segmental mobility of the molecular chains. This leads to a molecular configuration having a low segmental jumping frequency, which results in minimum permeability, good adhesion to metallic surfaces, and excellent hydrothermal stability.

A more recent study indicated that the enhancement of the hydrothermal stability of the composite depends strongly on three characteristics of the

* This work was performed under the auspices of the U.S. Department of Energy, Washington, D.C., under Contract DE-ACO2-76CH00016, and supported by U.S. Army Research Office Program MIPR-ARO-155-83.

Journal of Applied Polymer Science, Vol. 29, 2889–2920 (1984)
 CCC 0021-8995/84/092889-32$04.00
Published by John Wiley & Sons, Inc.

$CaO–SiO_2–H_2O$ system macromolecules formed within the polymer matrices[3]: (1) the morphological features and orientation of microcrystalline formations which act to reinforce the polymer matrices; (2) the mechanical strength of the crystallized compounds; and (3) the space-filling properties of the macromolecules, which form a dense agglomeration of filled matrix. For example, 11.3-Å tobermorite ($5CaO \cdot 6SiO_2 \cdot \times H_2O$) and calcium silicate hydrate (I) crystals produced from the hydrothermal reaction of hydraulic cement having a CaO/SiO_2 mole ratio of 0.54 greatly improve the hydrothermal stability of composites. The inclusion of xonotlite ($6CaO \cdot 6SiO_2 \cdot \times H_2O$), which has a specific needlelike microstructure, has been reported to increase the dynamic mechanical properties of films.[4,5] Conversely, poorly crystallized calcium hydroxide [$Ca(OH)_2$], formed within the polymer layers, had little if any effect on the ultimate strength of the composites.[6] From these observations, it was concluded that the hydrothermal stability of $CaO–SiO_2–H_2O$ systems formed during hydrothermal exposures at >100°C is due not only to the degree of crystallization and the shape of the microcrystal structure but also to the relatively high quantity of SiO_2 molecules existing in the hybrid hydration macromolecules. The results suggested that, when an anhydrous $CaO–SiO_2$ compound powder is to be used as a reactive filler with polymer blends, a hydraulic cement having a low mole ratio of CaO/SiO_2 should be employed.

The above findings indicate that the composite system can be utilized as a protective coating for metal surfaces exposed to hydrothermal environments. Failures of most conventional polymer films during exposure to aggressive hot water environments are likely to be due to (1) high segmental mobility of molecular chains, (2) low thermal relaxation of the polymers, (3) increase in hydrophilic groups, and (4) low dynamic mechanical properties. Each of these factors must be considered in attempting to provide the total protection needed for long service life in hydrothermal environments. Therefore, the physicochemical factors that determine the hydrothermal stability and the bounding characteristics of inorganic macromolecule–ionomer composite films have been investigated, and the results are given in this paper. These factors include the degree of polymer–filler interactions, thermodynamic properties, water transport properties, mechanical behavior, morphological features of the film surfaces, surface-free energy, interfacial adhesive strength, wetting behavior, and spreading kinetics.

First, several physicochemical properties of composite materials in thin films were assessed, and then the bonding characteristics at the composite–metal interface were investigated. The latter involve studies of the wetting behavior and the kinetics at modified metal surfaces by the resin blends and the possible interactions between the composites and metals.

EXPERIMENTAL

Materials

The methy methacrylate (MMA)-based polymer system used as a film-forming material consisted of a mixture of 57 wt % MMA monomer (DuPont Type EP-4160), 38 wt % bead PMMA (DuPont Elvacite 2008) with a mo-

lecular weight of $\sim 3 \times 10^4$, 5 wt % trimethylolpropane trimethacrylate (TMPTMA) crosslinking agent (Satamar Co., Ltd.). This resin blend had a viscosity of 217 cP and a surface tension (γ_{LV}) of 32.10 dyn/cm at 24°C. Since MMA–TMPTMA copolymers are glassy and brittle, the flexibility of the resin over the temperature ranges of interest was enhanced by incorporating a 10 wt % dibutoxyethyl phthalate (DBEP) plasticizer (C. P. Hall Co.). Polymerization of the plasticized MMA–TMPTMA resin was initiated by adding 3 wt % benzoyl peroxide (BPO) of 98% purity and 1 wt % *N,N*-dimethyl-p-toluidine (DMT) at an ambient temperature of 24°C. After mixing of all the ingredients, the gel time of the resin was ~10 min.

A commercial class J cement (Lehigh Portland Cement Co.) was used as a hydraulic-type reactive additive and a source of divalent metallic cations. This type of cement is frequently used in the completion of oil wells operating at temperatures > 110°C.[7] Its chemical constituents were as follows: CaO 40.68%, SiO_2 50.97%, Al_2O_3 0.86%, MgO 1.01%, Fe_2O_3 0.70%, and SO_3 0.29%; loss on ignition was 4.75%. Class J cement is characterized by its high silica content, which is needed to prevent strength retrogression at temperatures > 110°C.

Silica flour filler, which is generally used as a pigment in organic coatings, was used as a reinforcement in the films. The particle size of both the cement and the silica flour additives was < 200 mesh (0.074 mm).

The metal plates used in measurements of the tensile-shear lap joint bond for metal adhesives were polished with ultrafine emery paper. Microscopic measurements (× 400) revealed that the surface irregularities had maximum depressions of < 1.0 mil in depth. Immediately after polishing, the plates were scrubbed with a dry hand brush to remove any dust from the surfaces. Before film deposition, the plates were immersed in acetone for 24 h. To prepare the composite films, 50 parts of the initiated MMA–TMPTMA resin were added to 50 parts of the silica flour–class J cement filler. Six different ratios of silica flour to cement (100/0, 90/10, 80/20, 70/30, 50/50, and 30/70) were tested. After the two components were thoroughly hand-mixed for ~30 s, filled composite films with a thickness of 25–33 mils were cast on polyethylene sheets with a casting knife and then cured at room temperature for ~2 h.

Measurements

Measurements of the physicochemical factors were done on film and coating samples before and after exposure in an autoclave for up to 10 days at temperatures of 100°C, 150°C, and 200°C.

The glass transition temperature T_g of the polymer composites was measured with a DuPont 910 Differential Scanning Calorimeter (DSC) equipped with a DSC cell at a heating rate of 10°C/min under nitrogen gas flowing at a rate of 50 mL/min. The samples weighed 10–12 mg.

Tensile strength tests were done on dumbbell-like rigid composite film samples 70 mm long and 5 mm wide at the narrowest section. Stress–strain diagrams were obtained with a tensile tester having a crosshead speed of 0.5 mm/min. All strength values reported are for an average of three specimens. The changes in weight of the films after exposure were also measured as a function of time at the prescribed temperatures.

A Perkin-Elmer Model 257 Spectrometer was used for infrared analysis. The tests were performed by preparing KBr discs made by mixing 200 mg KBr and 3–5 mg of the powdered samples that had been crushed to a size of < 0.053 mm. The spectra were run at an 8 min scanning rate over the range of 4000–600 cm^{-1}.

Contact angle measurements on the film and metal surfaces were made with a contact angle analyzer. All measurements were made at 60% RH and 24°C within 30 s of drop application. Surface tension measurements were made with a Cenco-Du Nouy Tensiometer Model 70535.

A Ruska Liquid Permeameter was used for determining the water permeability of films ~25 mm in diameter and ~27 mil thick. The permeability measurements were made by determining the amount of water that is passed through the films under a pressure gradient of 2 atm for 2 h.

Microstructure deformation of the film surfaces caused by hot water attack was observed by scanning electron microscopy (SEM). The samples were prepared by depositing a gold film on the surface of composite films. SEM examination was also employed to identify the morphological features of the hydration compounds formed on the amorphous polymer layers. The samples were prepared the same way.

The lap-shear tensile strength of metal-to-metal adhesives was determined in accordance with the modified ASTM Method D-1002. Prior to overlapping between metal strips having dimensions of 50 mm length, 15 mm width, and 2 mm thickness, the 10 mm long by 15 mm wide lap area was coated with copolymer composite adhesive. The thickness of the overlapped film was 7–10 mils. The bond strength value of a lap shear specimen was the maximum load at failure divided by the total bonding area of 150 mm^2.

RESULTS AND DISCUSSION

Properties of Cast Composite Films

Glass Transition Temperature

High molecular mobility and segmental jumping frequency of the main chains of an amorphous polymer, during exposure to hot water, is one of the physicochemical factors affecting the hydrothermal disintegration of polymer films, caused by the chain scissions. It is therefore important to investigate the magnitude of the segmental immobilization in terms of the chain stiffness and the rigidity of the polymer molecules. Since the glass transition temperature T_g is a second-order temperature which can be regarded as the relaxation and motion of the major segments in the backbone molecular chains of an amorphous polymer,[8,9] the T_g of the polymer composites was determined as a means of estimating the degree of segmental mobility of the polymer molecules.

The influence of the hydrated inorganic macromolecules on the stiffness of the polymer chains was analyzed by comparing T_g values for the plasticized MMA–TMPTMA copolymer films containing mixed fillers with various ratios of silica flour (S) to hydralic cement (C). Differential scanning

calorimetry (DSC) at a heating rate of 10°C/min was used to determine the T_g of the samples. Typical DSC thermograms showing the essential features for film samples containing S/C ratios of 100/0, 90/10, 70/30, and 30/70, after exposure in an autoclave to water at 150°C for 24 h (Fig. 1) all have endothermic peaks between 57°C and 69°C. The T_g values were obtained from the endothermal peaks by finding the intersection point of the two linear extrapolations. The data indicate that use of an optimum amount of cement in the mixed filler consisting of silica and cement raises the T_g of the composite film after exposure to hot water. Samples containing filler with an S/C ratio of 70/30 had a T_g of 63°C, ~6°C higher than that at S/C = 100/0. Since the segmental immobilization of chains is directly related[10] to an increase in T_g, this apparently verifies that the macromolecules formed by hydraulic reactions of the cement in contact with hot water serve to restrict the segmental mobility of the main chains. The slight reduction in T_g at an S/C ratio of 30/70 indicates that the optimum concentration of cement in the filler is between 30% and 70%.

Tensile strength and T_g data, as a function of S/C ratio for the composite films after exposure to water at 150°C for 24 h, are given in Figure 2. The T_g rises with increasing cement content until it reaches a maximum of 63.5°C at an S/C ratio of 50/50.

The curve for the tensile strength of the film as a function of the S/C ratio is similar to that for T_g. The data indicate that the strength increases with S/C ratio between 100/0 and 70/30, and then decreases. The ultimate strength, 1150 psi, for copolymer films with a mixed filler having an S/C ratio of 70/30 was ~70% higher than that of films with a silica flour filler lacking cement.

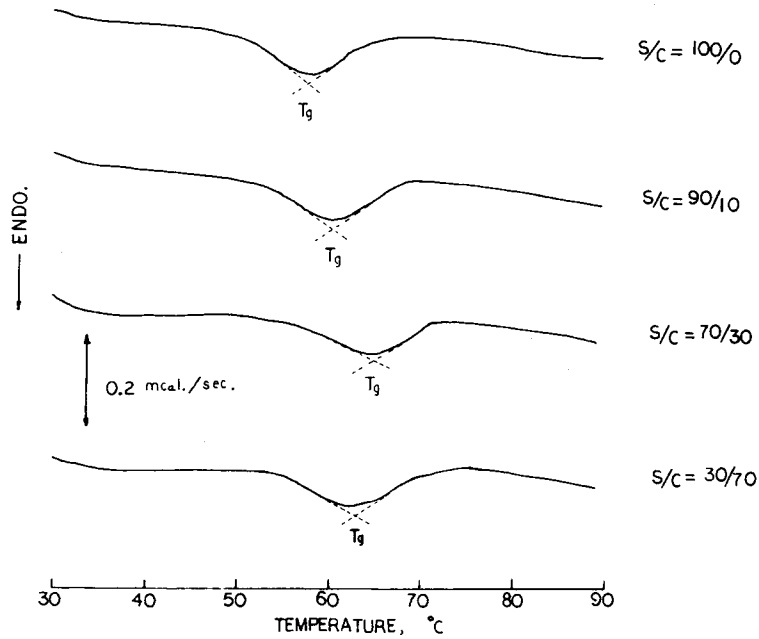

Fig. 1. DSC thermograms of MMA–TMPTMA copolymers having fillers with various S/C ratios, after exposure for 24 h to water at 150°C.

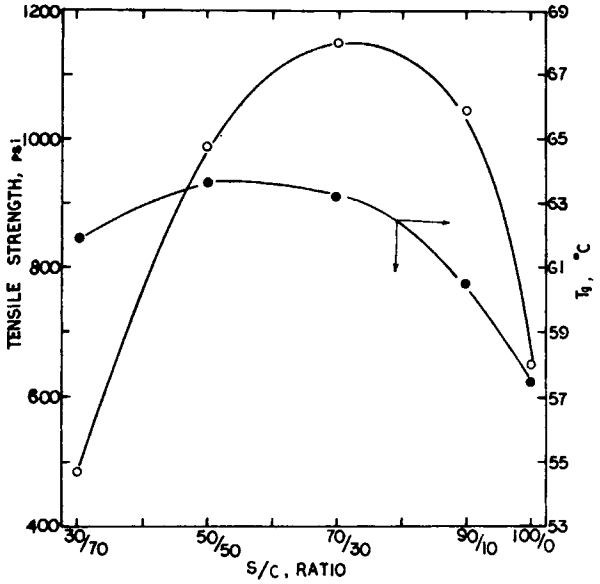

Fig. 2. Tensile strength and T_g of films as a function of S/C ratio after exposure to water at 150°C for 24 h.

Many recent investigations[11-13] have shown that the influence of T_g behavior on filled polymers depends mainly on the segmental adsorption and orientation of the main chains in the immediate vicinity of the filler surface. These can result in strong filler–polymer interactions and agglomeration forces. Strong filler–polymer interfacial forces also contribute to the enhancement of the mechanical strength of composite materials. However, the newly produced formations at the interface between the configurated macromolecules and the polymer chains not only yield strong agglomerations and chain entanglements but also are likely to produce increased interfacial stresses which result in chain enlargement occurring along with the growth of the macromolecules. Therefore, the reductions in film strength as the S/C ratio is decreased can be interpreted as being due to extraordinary chain enlargement, which exerts a "squeezing" force on the larger macromolecules formed on the polymer layers. These high interfacial stresses can be reduced by the formation of microcracks between the polymer matrices and the macromolecules. In fact, for copolymer films containing a filler with a S/C of 30/70, and having a decreased T_g of 61.5°C, the tensile strength was down to 480 psi, which resulted in deformation and microcracking of the films. These results suggested that the optimum amount of reactive cement must be used with the silica flour in the filler to prevent film strength reduction due to squeezing deformations.

The changes in weight of the composite films after immersion in water at 150°C for periods of up to 10 days were also measured (Fig. 3). The control samples (S/C = 100/0) showed weight loss throughout the exposure, up to ~15% after 10 days; they also showed many blisters on their surfaces. In contrast, the films with mixed fillers containing cement and silica flour increased in weight. Samples with S/C 70/30 filler increased in weight

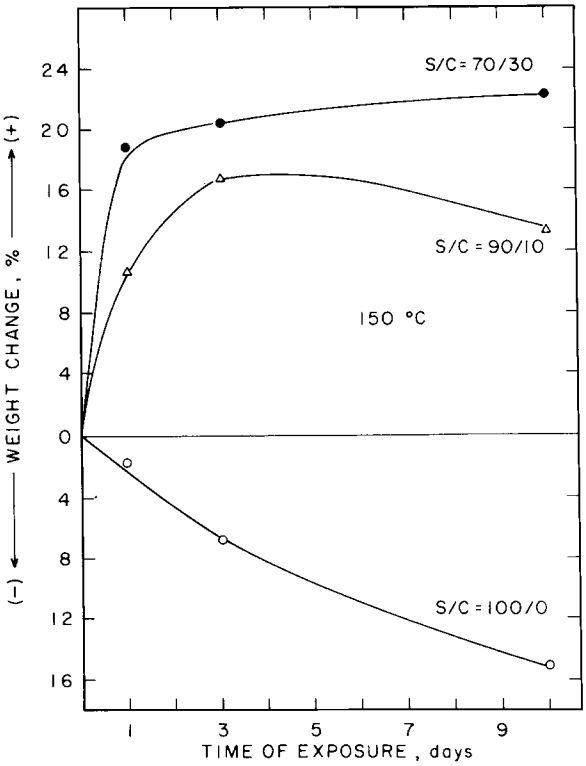

Fig. 3. Film weight changes after exposure to water at 150°C.

rapidly over the first 24 h, and then more gradually for the duration of the 10-day exposure. This was due to conversion of the cement grains in the copolymer matrix into hydrated cement compounds based on the $CaO–SiO_2–H_2O$ system during exposure to hot water. The film surfaces showed little or no blistering.

Samples with S/C 90/10 filler, when exposed for 10 days to the hydrothermal environment, increased in weight for ~3 days and then gradually decreased, but they showed no evidence of deterioration or corrosion.

Unfilled and filled copolymer films that had been kept in an autoclave at 200°C for 10 days were visually inspected to determine changes in appearance and color, and the degree of deformation. Samples from some of these studies are shown in Figure 4. After a 10-day exposure, the unfilled bulk copolymer films were severely attacked and changed beyond recognition. The film with silica flour filler (S/C 100/0) showed attack at a lower rate, and changes in color. This film exhibited considerably more deterioration than the films containing the cement additive. Increased resistance with increased cement content was apparent.

IR Studies

Infrared (IR) absorption spectroscopy was used to elucidate the role of cement additives as a means for improving the hydrothermal stability of MMA–TMPTMA copolymer containing carboxyl groups (O=C—O—R) in

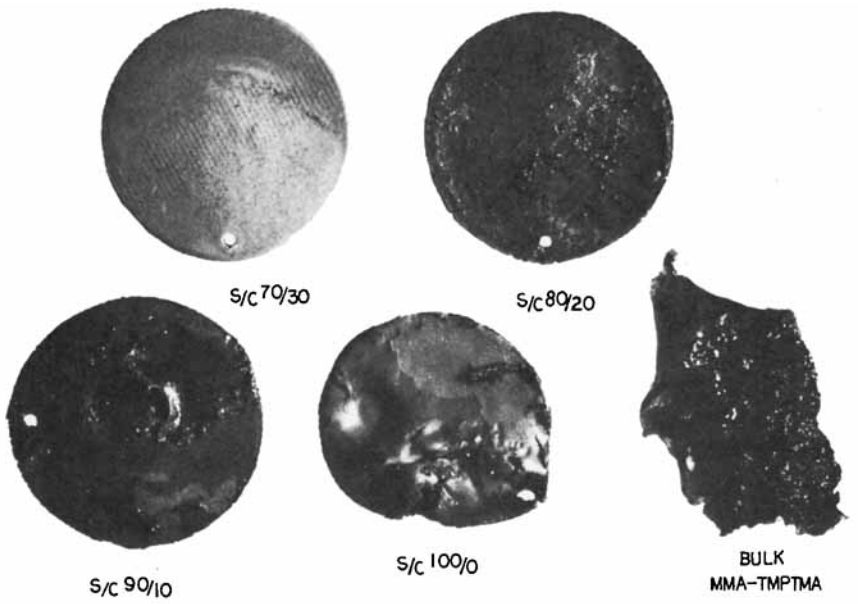

Fig. 4. Comparison of hydrothermal attack by hot water on various filled copolymer films.

the side chains. To prepare the samples, films exposed to hydrothermal conditions for 10 days (see Fig. 4) were first dried in an oven at 100°C for 24 h and then ground to a particle size <0.0074 mm.

Earlier work[1] had shown that hydrothermal deterioration of polymers, caused by the hydrolysis of a pendent carboxyl group, can be restrained by ionic crosslinking initiated by the strongly nucleophilic Ca^{2+} ions released from cement during contact with hot water. A salt bridge consisting of —COO^-—Ca^{2+}—^-OOC complexed formulations, resulting from ionic bonding between the Ca^{2+} ions and the carboxylate anions (COO^-) from the hydrolysis of carboxyl groups, has been confirmed by asymmetrical and symmetrical stretching vibrations at 1540 and 1398 cm^{-1} in the IR spectrum. In addition, a correlation between the reduction in absorbance of the carbonyl groups at 1710 cm^{-1} and the increasing intensity of $COO^-(Ca^{2+})$ complex groups at 1540 and 1398 cm^{-1} suggested the possibility of measuring the rates of conversion to carboxylate anions. Accordingly, the degree to which ionic Ca^{2+} complex salt formations affected the restoration of hydrothermal degradation was assessed on the basis of the shifts in IR frequency and the changes in band intensity at 1710, 1540, and 1398 cm^{-1}.

The test results from these samples (Fig. 5) show that the intensity of the $COO^-(Ca^{2+})$ frequency at 1540 and 1398 cm^{-1} increases as the cement content of the filler increases. Conversely, the band of carbonyl groups at 1710 cm^{-1} tends to shorten with growth of the $COO^-(Ca^{2+})$ bands. These results verify that the carboxylate anions, produced by hydrolysis of the pendent carboxyl groups in the copolymer molecules, are converted into $COO^-(Ca^{2+})$ groups by the nucleophilic Ca^{2+} ions released from cement grains during exposure to hot water. Since an increment of salt bridge formations per molecule results in an abundant supply of Ca^{2+} ions, the optimum amount of cement additive should be used to provide a source of

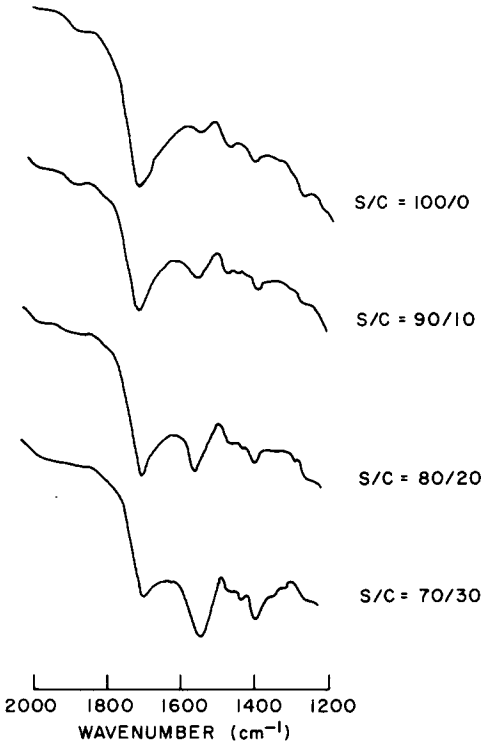

Fig. 5. Shift in IR frequency as a function of S/C ratio at 200°C.

Ca^{2+} ions for inhibiting polymer chain scission caused by the hydrolytic decomposition of the pendent groups.

The rate of reaction between the Ca^{2+} ions and the COO^- anions as a function of hydrothermal temperature, from 50°C to 200°C, was quantitatively estimated by comparing the absorbance ratios of the $—COO^-(Ca^{2+})$ groups at 1540 cm^{-1} and the C=O groups at 1710 cm^{-1}. Samples containing a filler with an S/C ratio of 70/30 were used in the IR spectrophotometry analysis. Prior to testing, the films were exposed for 10 days to water at temperatures of 50°C, 100°C, 150°C, and 200°C.

In IR quantitative analysis, the peak height or the area of the band is taken as the criterion of bank intensity. Therefore, an accurate measurement of band intensity is very important. The absorbances of two peaks were determined as the distance from the absorption maximum to a baseline connecting the two wings of the band.

A plot of the absorbance ratio as a function of temperature (Fig. 6) shows a direct linear relationship. This implies that the intensity of the band characteristic of $COO^-(Ca^{2+})$ formation becomes stronger as the C=O group band intensity decreases. Accordingly, it appears that a large number of pendent carboxyl groups are converted into carboxylate anions by the hot water. These anions simultaneously produce Ca^{2+} salt bridge structures (formed by ionic reactions with the Ca^{2+} ions) which play an essential role in binding the COO^- ions. The data also suggest that the rate of ionic bonding through salt formation is directly related to the temperature up

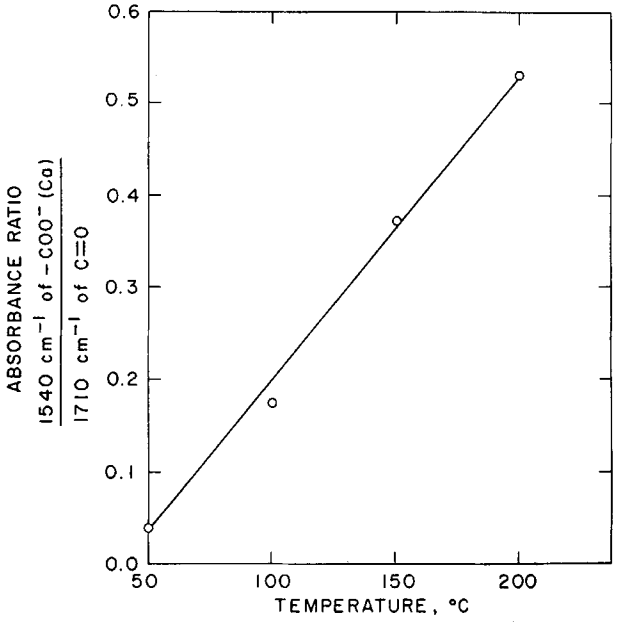

Fig. 6. Relationship between absorbance ratio and hydrothermal temperature for film containing filler with an S/C ratio of 70/30 after exposure to hot water for 10 days.

to 200°C and to the quantity of cement mixed with the silica flour filler. The absorbance ratio of 0.55 at 200°C seems to indicate that >50% of the carboxyl groups were changed in the Ca salt formations. This is ~18 times as large as the percentage for samples at 50°C.

Three possible molecular structures for the calcium carboxylate complexes can be deduced. These are shown below:

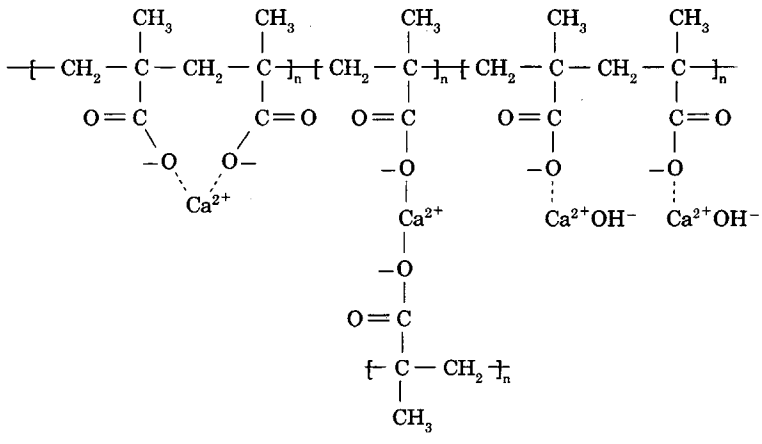

Complexed structure (I) is characterized as an intramolecule hydrated salt type formed within the single chain, and (II) refers to an intermolecule hydrated salt type through the crosslinking structure which connects two adjacent carboxylates between the chains. The calcium cation in a salt

bridge will be stabilized by six water molecules to give an octahedral structure.[14] The neutral H_2O molecules coordinated to the Ca^{2+} ions will be stable enough to remove water vapor from ordinary air at ambient temperature.[15] An alternative formation (III) may be interpreted as a pendent half-salt.

Assuming that the Ca-complexed ionomer matrix consists of the above three species, formations (I) and (II) contribute significantly to enhancement of the chain stiffness, lower the degree of free rotation of the chains, and increase the chain entanglements, thereby increasing T_g levels and the mechanical strength of the films.[16] On the other hand, the half-salt located in the pendent groups may be presumed to have little if any effect on restraining chain rotation. With regard to half-salt molecular structures, $—COO^-—Ca^{2+}OH^-$ groups containing an interchangeable hydroxyl group are more likely to be hydrophilic than hydrophobic.

Thermal Behavior Analysis

The enhanced thermal stability of Ca-complexed compound films was assumed to be due mainly to the presence of a larger number of salt bridge formations and to the hydrated inorganic macromolecules formed during exposure to the hydrothermal environment. Thermal measurements intended to clarify this assumption were made by using thermogravimetric and differential thermal analysis (TGA and DTA). Since the numbers of salt formations and of hybrid macromolecules increase with increasing hydrothermal temperature, copolymer films with S/C 30/70 filler were exposed for 3 days to water at temperatures of 24°C, 150°C, and 200°C. After exposure, the thermal behavior analyses were performed at a heating rate of 10°C/min in nitrogen gas.

The TGA thermograms are shown in conjunction with the DTA curves in Figure 7. The TGA curve for the samples exposed at 24°C (the controls) indicates that weight loss began at ~225°C. It reached 13% at ~275°C and 40% at ~400°C. These temperatures correspond to weak and strong endothermic peaks on the DTA curve. The former peak may be due to the rotational energy of the molecular chains and the latter to the integrated heat of fusion.

In contrast to the controls, which lost no weight up to ~225°C, the samples that had been exposed to water at 150°C lost ~0.13 g over the temperature range 80–200°C. This appears to be directly related to the two weak DTA endothermal peaks at 80°C and 175°C. The peak at ~80°C is attributed to vaporization of free water. The total amount of free water was calculated from the TGA data to be ~0.03 g. This corresponds to ~0.26% by weight of the total composite mass.

The weight loss at ~175°C may be due to thermal dissociation of bound water, including the gel water combined with the hydraulic cement and the neutral H_2O molecules coordinated to Ca^{2+} ions in Ca^{2+} bridges. The amount of bound water was calculated to be ~0.1 g. The onset temperature for thermal decomposition of the 150°C sample was ~330°C, ~105°C higher than that of the control. The DTA curve shows that the intensity of its endothermal peak at ~300°C is much weaker than that for the control. This may imply that the chain rotation energy, which can be determined

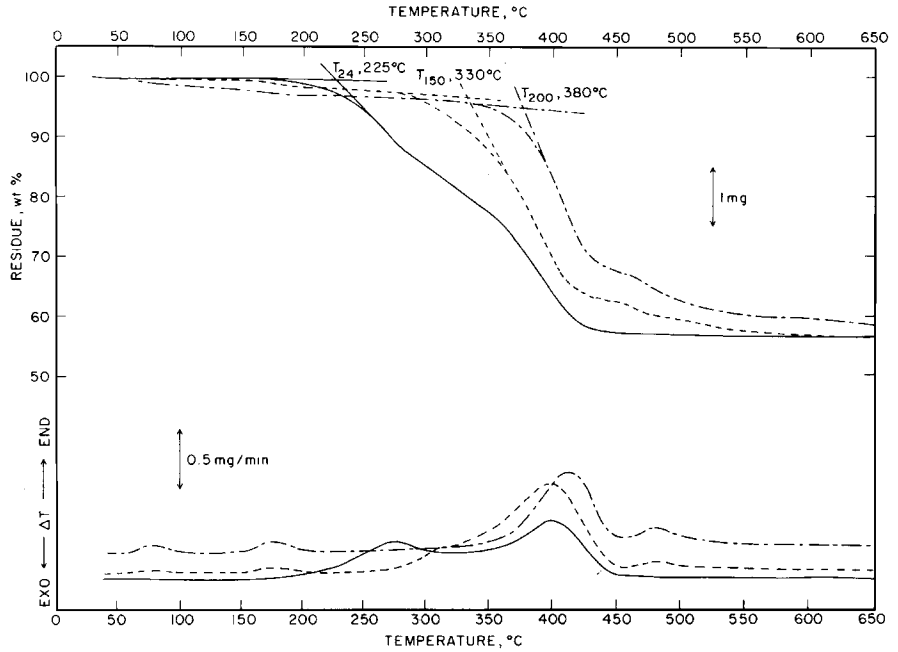

Fig. 7. TGA and DTA curves for copolymer films with S/C 30/70 after exposure to water at temperatures of 24°C (——), 150°C (—), and 200°C (---).

from the total area of the curve enclosed by the baseline, was reduced by the formation of salt complexes and by the inorganic macromolecules produced during the hydrothermal exposure.

Another weak peak appears in this curve at 480°C. This is due[17] to the dehydration of $Ca(OH)_2$ and is related to the slight weight loss between 480°C and 540°C on the TGA curve. The $Ca(OH)_2$ formation of ~0.15 g was calculated on the basis of the distance between the onset of the two linear portions before and after the transition period, on the TGA curve. It amounts to ~3.72% by weight of anhydrous cement used.

The sample that had been exposed to water at 200°C lost ~0.18 g of water between the temperatures 50°C and 110°C. The slight change in the slope of its TGA curve near 150°C is due to the presence of ~0.16 g of bound water, which is ~60% greater than that in the samples exposed at 150°C.

It is well known that the amount of water in a well-hydrated cement retained at 105°C is generally ~20% by weight of the anhydrous cement.[18] Thus, if ~0.16 g of bound water is assigned to the hydrated cement, this corresponds to ~4.1% by weight of the total anhydrous cement mass. It may, therefore, be interpreted that ~21% of the cement present in the copolymer matrix was completely hydrated. However, since some H_2O molecules coordinated to Ca^{2+} ions should also be contained as bound water, the amount of hydrated cement is actually $<21\%$. These results seem to suggest that the hydration products of cement are probably formed in a very thin superficial layer on the films, where they seem to protect the organic polymer from hydrothermal deterioration. On the other hand, the onset temperature of the major weight loss, as determined by TGA, was

~380°C. This was accompanied by a prominent endothermic peak at 425°C on the DTA curve. The high onset temperature, 50°C above that for the 150°C samples, seems to verify that the configurative combination between the highly formed salt complexes and the macromolecules contributes significantly to the improvement in the hydrothermal stability of the composite films. The temperature at which the film exhibited a 40% weight loss was ~600°C. DTA data also indicated the disappearance of the exothermal peak at ~300°C. Therefore, it appears that these formations enhance chain stiffness. On the basis of the change in the TGA slope at ~470°C, the amount of $Ca(OH)_2$ produced was estimated to be ~0.2 g, which corresponds to ~5.1% by weight of the anhydrous cement.

Water Permeation

Water permeation through the composite films is one of the most important properties of films designed for protective coating applications. The permeability of the film samples was measured by forcing pressurized water through 28-mm-diam samples, ~27 mil thick. Samples in this test series contained fillers with S/C ratios of 100/0, 90/10, 70/30, and 30/70, and were exposed in an autoclave for 3 days at temperatures ranging between 100°C and 150°C. The water permeability at pressures up to 2 atm was computed by using the following formula:

$$K_a = \mu VL/AP$$

where K_a is the permeability (darcys) of the sample (intrinsic permeability), V (cc/s) is the rate of flow at the fluid viscosity μ (cP),and L and A are the thickness (cm) and the cross section area (cm^2) of the sample under the hydrostatic pressure P (atm).

For all calculations a constant of 8.141×10^{-2} was derived for a driving pressure of 2.0 atm, a surface area of 6.154 cm^2, and a viscosity at 20°C of 1.002 cP. Hence, the intrinsic permeability K_a is defined by $K_a = 8.141 \times 10^{-2}\ VL$ (Darcys).

Test results from these film samples (Table I) show that the water permeability is highly dependent on the autoclave temperature. For films exposed at 100°C, the permeability value increased slightly as the S/C ratio was decreased. The results for films exposed at 130°C were interesting: the permeability was lowered by increasing the cement content up to S/C ratios

TABLE I
Water Permeabilities of Films after Exposure for 3 Days in an Autoclave at 100°C, 130°C, and 150°C

S/C ratio	Water permeability (darcys)		
	100°C	130°C	150°C
100/0	6.24×10^{-8}	9.38×10^{-8}	1.52×10^{-7}
90/10	6.60×10^{-8}	8.55×10^{-8}	1.09×10^{-7}
70/30	6.72×10^{-8}	8.04×10^{-8}	9.85×10^{-8}
30/70	7.15×10^{-8}	9.10×10^{-8}	2.38×10^{-7}

of 70/30, going from 9.38×10^{-8} darcys for S/C = 100/0 to 8.04×10^{-8} darcys for S/C = 70/30, but was raised by further increase in cement content. Earlier data for tensile strength showed similar trends (see Fig. 2).

Samples exposed in the autoclave at 150°C produced similar results. The films with S/C = 70/30 filler had the lowest intrinsic permeability, 9.85×10^{-8} darcys, 35% less than that for S/C = 100/0.

Permeability increased with exposure temperature. The permeability of films with S/C = 70/30 filler exposed at 150°C was 47% higher than that of those exposed at 100°C, and for films without cement this increase was 143%. This seems to support the theory that the hydrated macromolecules distributed randomly on the surface of an amorphous copolymer matrix are probably responsible for minimizing the permeability of the organic films to water.

The finding (mentioned earlier), that after exposure at 105°C, films containing a high concentration of cement (S/C = 30/70), had a much higher permeability than did the controls (S/C = 100/0), appears to indicate that deformation due to the presence of superfluous macromolecules has a stronger influence on the permeability of the films than does hydrothermal deterioration of the copolymer matrices. The higher water permeability is due to the open structures created by the deformation results.

To obtain further information about the effects of cement additives on water permeability, other physicochemical factors that affect water permeability, including surface wettability, surface free energy, and surface texture were assessed by using a contact angle indicator and a scanning electron microscope (SEM).

Wetting Behavior of Film Surface

Since the wettability relationship between water and a solid surface is considered to be a type of complex water–solid interaction,[19] the magnitude of the water wettability of a plane film surface can be estimated from the value of the work of adhesion, W_A (H_2O), which is a generally useful index of surface wetting. The value of W_A (erg/cm^2) was calculated by using the well-known classical expression originated by Young[20] and Dupre,[21]

$$W_A(H_2O) = \gamma_{LV}(1 + \cos\theta) + \pi^s,$$

where γ_{LV} (dyn/cm) is the surface tension of water at 24°C, θ is the average value of the measured contact angle on the solid surface, and π^s is the equilibrium spreading pressure of the adsorbed vapor on the solid. In many approaches to the theory of contact angles, π^s has been assumed to be approximatedly zero.[22] Fox and Zisman[23] showed that $\gamma_{LV}(1 + \cos\theta)$ was a good approximation for W_A, the work of adhesion between liquid and solids which do not wet.

The film samples, containing fillers with various S/C ratios, that were used for contact angle and SEM measurements were exposed in hot water for 3 days at temperatures up to 150°C and then rinsed several times with distilled water and dried in the oven at 70°C for 24 h. All the measurements were made at a temperature controlled at 24.0 $\pm$ 0.1°C, and 50% relative humidity. In measuring contact angles, because the angles on the dry film

surfaces gradually increased during the first 10–20 s, the static angles were recorded after the boundary of a sessile drop had been allowed to equilibriate for 30 s after deposition.

A plot of W_A as a function of S/C ratio for films exposed at temperatures of 24°C, 100°C, and 150°C (Fig. 8) shows that W_A is affected both by hydrothermal temperature and by S/C ratio. The W_A values for all samples exposed at 24°C were essentially constant, varying only from 83.0 to 85.9 erg/cm^2, showing that these films, which have a smooth surface, have a relatively low magnitude of surface wettability. In contrast, for the samples exposed in boiling water at 100°C, the W_A value rose sharply at S/C ratios $>70/30$, going up to 113.6 erg/cm^2 for noncement-containing control samples. This value was 31.3% higher than that for the sample with S/C 70/30 filler, and 32.9% higher than that obtained from the same film surface at 24°C. The results suggest that the increase in surface wettability with lower cement concentration is probably due to an increase either in the number of hydrophilic groups or in their accessibility to water. The finding that W_A at S/C = 30/70 was almost the same as at S/C = 70/30 seems to demonstrate that the presence of $>30\%$ cement by weight of the total mix filler results in a low surface wettability.

The W_A plot in Figure 8 for films exposed at 150°C showed an interesting variation: the degree of wetting decreased sharply with increased cement concentration between S/C ratios of 100/0 and 70/30, and then increased somewhat with further lowering of the S/C ratio. The decrease in wettability in the S/C range of 100/0 to 70/30 is similar to the trend seen with the 100°C samples. The surface of the control samples had a W_A value of 120 erg/cm^2, and the lowest value (90 erg/cm^2) was for the samples with S/C 70/30 filler. A possible reason for the increased wettability of films with S/C 50/50 (and lower) fillers is enhancement of the surface roughness by

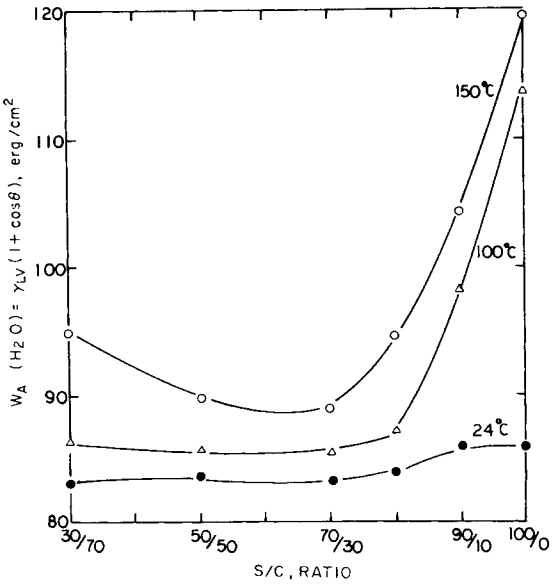

Fig. 8. Work of adhesion (water) vs. various S/C ratios at temperatures of 24°C, 100°C, and 150°C.

squeezing deformation of the films resulting from the increased concentration of hydration macromolecules in the amorphous copolymer matrix.

This can be further clarified by studying the relationship between cos θ and the IR absorbance ratio for the COO^-(Ca) at 1540 cm^{-1} frequency and the C=O groups at 1710 cm^{-1}. For samples that had been exposed to hot water at 150°C (Table II), the tendency for the absorbance ratio to increase as the S/C ratio decreases is in agreement with that obtained from films exposed at 150°C. This implies that the hydrophilic carboxylate groups formed by hydrolysis of the carboxyl groups present in the polymer molecules are converted into hydrophobic Ca-complexed salt formations by ionic reactions with free Ca^{2+} ions released from the cement grains in an aqueous medium. Thus, reaction of the abundant Ca ions available from larger amounts of cement is thought to make the polar film surface less hydrophilic and more hydrophobic. On the other hand, cos θ decreased as the cement quantity was increased from S/C 90/10 to 70/30 and then increased gradually with further decreases in the S/C ratio. In spite of being hydrophobic, the film surfaces may have enhanced wettability between S/C 50/50 and 30/70 because of heightened surface roughness and enlargement of their microcracking spaces. The latter results from the high internal stress concentration developed during growth of large hydrated macromolecules, which allows the transportation of more water.

To support the data on the wetting behavior, the surface free energy for the exposed film samples was determined by methods developed by Owens and Wendt[24] and Baszkin and Ter-Minassian-Saraga,[25] which are especially applicable to the surface characterization of polymers. Film surfaces that have high contact angles lack affinity for water and have a lower surface energy. Therefore, surface energy is one of the important factors affecting water permeability.

In measuring the total solid surface-free energy γ_S, it is assumed that γ_S is the sum of two components: the dispersion forces γ^d and the dipole–hydrogen bonding forces γ^p. The geometric mean equation, proposed as a natural extension of the Fowkes[26] empirical formula by Owens and Wendt,[24] was used to estimate these energy contributions for the high surface-energy systems:

$$\gamma_{SL} = \gamma_S^0 + \gamma_{LV} - 2\sqrt{\gamma_S^d \gamma_L^d} - 2\sqrt{\gamma_S^p \gamma_L^p} \quad (1)$$

TABLE II
Variation of Contact Angle and Absorbance Ratio as a Function of S/C Ratio for Samples Exposed at 150°C

S/C ratio	Cos θ (water)	Absorbance ratio, 1540 cm^{-1} of COO^- (Ca) / 1710 cm^{-1} of C=O
90/10	0.43	0.043
80/20	0.30	0.081
70/30	0.22	0.104
50/50	0.24	0.136
30/70	0.31	0.142

where γ_{SL} is the interfacial tension at the solid–liquid interface, γ_{LV} is the surface tension of liquid on a free surface energy γ_S^0 of the solid while under vacuum, and γ_S^d γ_L^d and γ_S^p γ_L^p refer to the dispersion forces and polar forces in the solid and the liquid. Generally, equilibrium at the solid–liquid interface depends on the four parameters governed by the following Young's expression:

$$\gamma_{LV} \cos \theta = \gamma_S^0 - \gamma_{SL} + \pi^s \tag{2}$$

In dealing with the adhesion of a liquid on a perfectly flat solid surface, the free energy of work of adhesion W_A is given by

$$W_A = \gamma_{LV}(1 + \cos \theta) + \pi^s \tag{3}$$

By assuming that $\pi^s = 0$ for eqs. (2) and (3), these equations can be combined and written as follows:

$$W_A = \gamma_{LV} + \gamma_S^0 - \gamma_{SL} \tag{4}$$

Accordingly, eq. (1) can be reduced to the general form

$$W_A = 2\sqrt{\gamma_S^d \gamma^d{}_L} + 2\sqrt{\gamma_S^p \gamma_L^p} \tag{5}$$

In eq. (5), the values of γ_S^d and γ_S^p, which are needed to obtain the total solid surface energy γ_S, are unknown. They can be determined by the method of Owens and Wendt[24] by measuring the contact angles with water (H_2O) and methylene iodide (CH_2I_2). The latter is used because its molecules are much larger than H_2O[27] and therefore cannot duffuse into the pores between the hydrocarbon chains in the film. Values of W_A for water and methylene iodide were computed from experimentally measured contact angle and surface tension values. Values for the parameters γ_L^d and γ_L^p were obtained from data reported by Fowkes[28]: $\gamma_L^d = 21.8$ erg/cm^2 and $\gamma_L^p = 51.0$ erg/cm^2 for water; $\gamma_L^d = 48.5$ erg/cm^2 and $\gamma_L^p = 2.3$ erg/cm^2 for methylene iodide.

Figure 9 shows γ_S^p, γ_S^d, and γ_S values plotted as a function of S/C ratios for composite films after autoclave exposure at 100°C and 150°C. The values for γ_S^p at 100°C and 150°C are essentially independent of S/C ratio between 30/70 and 70/30 and then increase with decreasing cement content. The highest γ_S^p value obtained from the non-cement-containing control samples indicated that the surface is composed of a hydrophilic monolayer of oriented polar groups. Conversely, the lower γ_S^p values correspond to a polar surface with a lower hydrophilic density. The shift in γ_S^d for the surfaces of samples autoclaved at 150°C indicated a trend similar to that for the W_A results discussed previously.

Values for γ_S^d were lowest at a 70/30 ratio and then increased rapidly with a further decrease in cement content. The changes in γ_S^d occurring between S/C ratios of 70/30 and 30/70 are considerably higher (48.4% vs. 6.6%) than those for γ_S^p. This suggests that γ_S^d for high surface-energy solid film surfaces is more likely to be associated with surface roughness than with the inclination to polarizability of molecules. It should also be noted

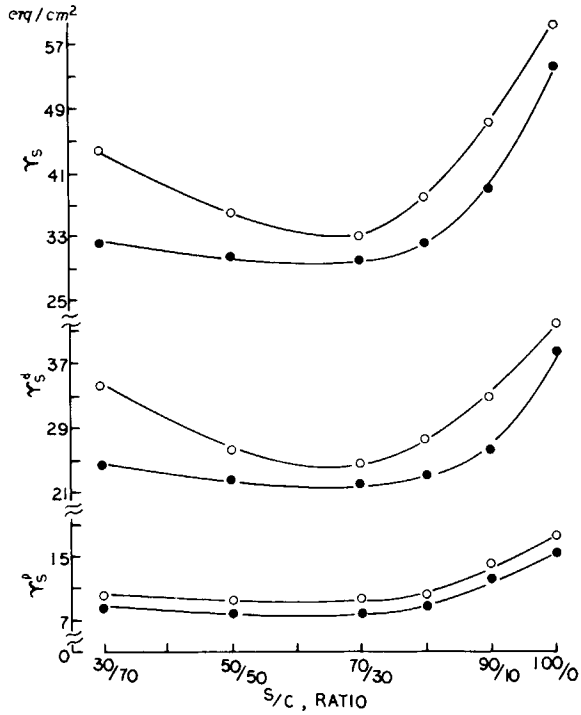

Fig. 9. Components of surface free energy as a function of S/C ratio for samples autoclaved at 150°C (○) and 100°C (●).

that, over a wide range of S/C ratios, the variation in γ_S^d at 100°C is relatively small. Thus, the use of cement as a method for increasing hydrothermal stability of films seems to be most effective at ~100°C.

Since the total surface free energy γ_S is the sum of the attraction forces γ_S^p and γ_S^d, its curve is similar to that for γ_S^d. The surface energies for the control, from the curve in Figure 9, were 53.61 erg/cm² at 100°C and 58.78 erg/cm² at 150°C, ~70% higher than those for samples with S/C 70/30 filler.

The above results indicate that the hydrolysis of the pendent carboxyl groups in the superficial layer of the film enhances either the number or the accessibility of the hydrophilic groups formed from the functional carboxylate groups previously detected by IR. Furthermore, the increased roughness of the film surface due to the hydrothermal deterioration of polymer matrices and the presence of extraordinarily formed inorganic macromolecules significantly increase water wettability and thus allow the transportation of more water.

Scanning electron microscopy (SEM) is the best approach to characterizing the morphological features of the material surfaces. The microstructure and morphology of the composite film surfaces, before and after exposure to hot water at 150°C for 3 days, were studied by this technique. Figure 10 (× 102) shows a surface of an unexposed bulk copolymer film without any fillers. Its surface morphology is smooth, and evidence is lacking as to whether the microcracking in the middle is caused by shrinkage

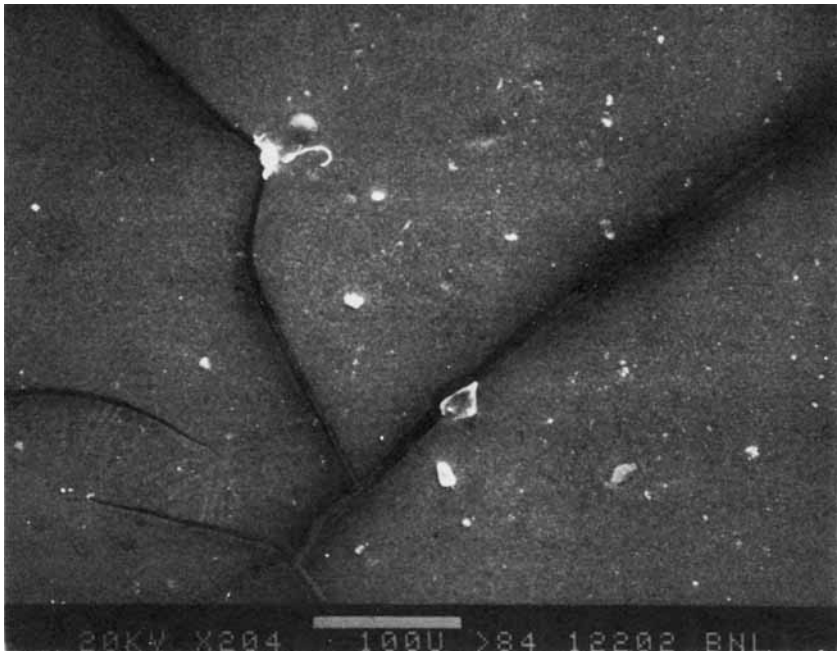

Fig. 10. Smooth surface of bulk MMA–TMPTMA copolymer before exposure in an autoclave.

of the copolymer or by deposition of gold film on its surface. Exposure to hot water caused dramatic changes (Fig. 11). The polymer molecules were strongly agglomerated by entanglement of the chain caused by severe hydrothermal deterioration, and resulting in increased surface roughness. The agglomerate particles consist of approximately spheroidal and spherical granules of ~40 μm diameter. Since the amount of coalescent polymer aggregation is thought to increase progressively with extended exposure time, some of the agglomerate particles may be naturally removed from the material surfaces, which would reduce the weight of the films.

An exposed copolymer film with silica flour filler (Fig. 12) had a heterogeneous solid surface exhibiting different areas with largely agglomerated polymer spheroids (A) and sharply protruding silica surfaces (B). The agglomerate particles appear very similar to those observed on the surface of the exposed homogeneous polymer. The roughness of this film surface indicates that the continuous copolymer layer formerly coating the surface of the silica grains was removed during the autoclave exposure. This surface texture results in increased surface-free energies, weight loss, and water wettability. Figures 13 and 14 show the surface textures of films with S/C 80/20 filler before and after exposure in the autoclave. The former is characterized by a continuous layer of copolymer coating the surface of the original cement and silica flour grains. The anhydrous cement grains cannot be distinguished by their appearance. After exposure, some small pits were detectable, but in general the surface was much smoother than that of the exposed film with silica filler. This morphology verifies that the hydraulic cement prevents severe deterioration of the polymer by the attack of hot

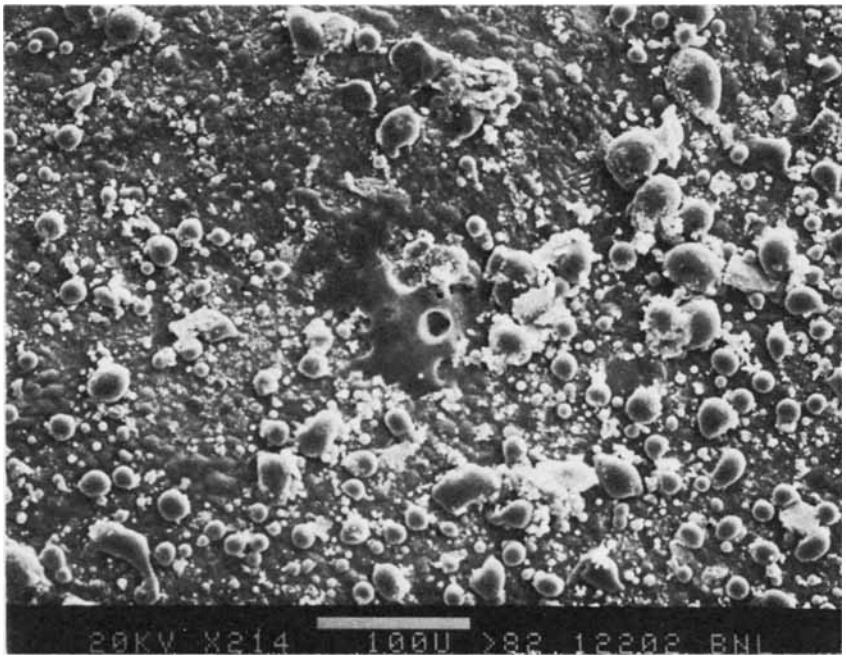

Fig. 11. Micrograph of copolymer granule agglomerated during exposure for 3 days to water at 150°C.

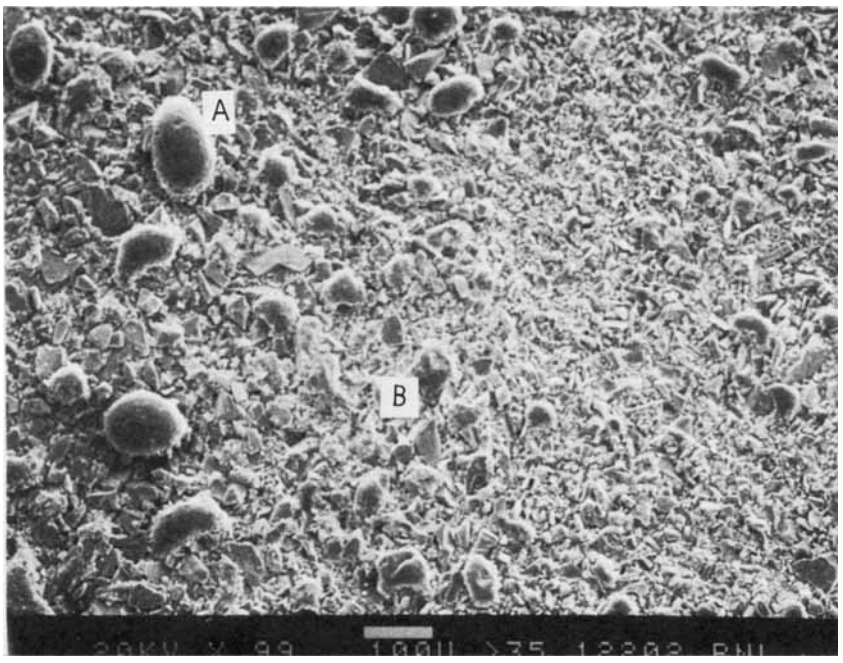

Fig. 12. Rough surface of copolymer film with silica flour filler after exposure to hot water.

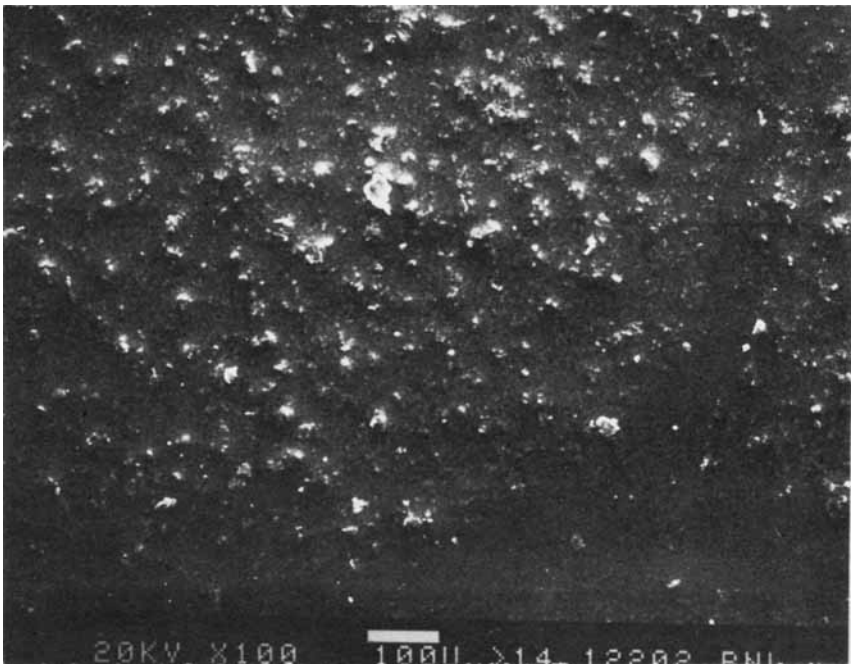

Fig. 13. Surface of copolymer film with S/C 80/20 filler before exposure.

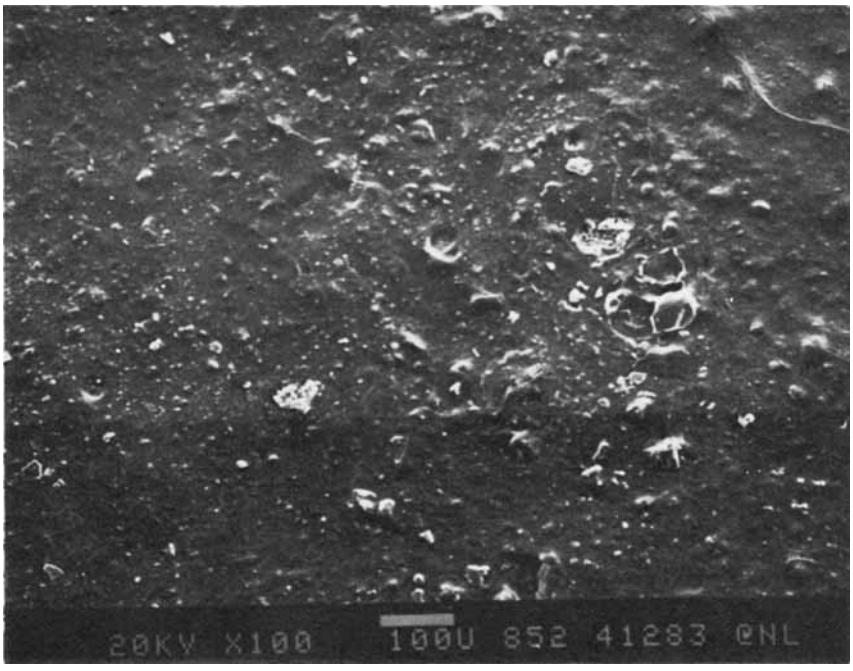

Fig. 14. Surface of film with S/C 80/20 filler after exposure to hot water.

water. Although at low magnification the surface appeared smooth, enlargement to × 2500 disclosed that a number of knobs had develop on the surface (Fig. 15). This may have been caused by the internal stress associated with the hybrid compounds of superficially formed Ca-complexed ionomer and hydrated cement macromolecules. The improvement of the hydroermal stability of copolymer matrices by cement additives is apparent from the microstructure of film containing a large amount of cement. At a low magnification (× 24) the surface texture of a film with S/C 30/70 filler after autoclave exposure (Fig. 16) shows numerous small cracks, in contrast to the agglomerated copolymers and silica particles seen on the films with silica filler (Fig. 12). Formation of the Ca-complexed ionomer, which would be expected to be stable at ~150°C, is thought to have prevented agglomeration of the copolymer. The cracking may be due to shrinkage of the hydrated cement macromolecules. This suggests that the superfluous cement contributes to surface roughness and thus increases surface free energy and wettability. Two different phases are seen in Figure 16, circular depression portions (C) and rough areas (D). The former are probably representative of the fresh composite surfaces disclosed by removing parts of a superficial layer of the Ca-complexed ionomer combined with the cement macromolecules. At a higher magnification (× 102, Fig. 17) the features of the hypodermically existing fresh surface are morphologically very similar to those of the exposed films with S/C 80/20 filler which are characterized by a continuous layer of copolymer molecules (Fig. 14). This seems to verify that the superficially formed inorganic macromolecule-complexed ionomer layers contribute significantly to the hydrothermal stability of the film.

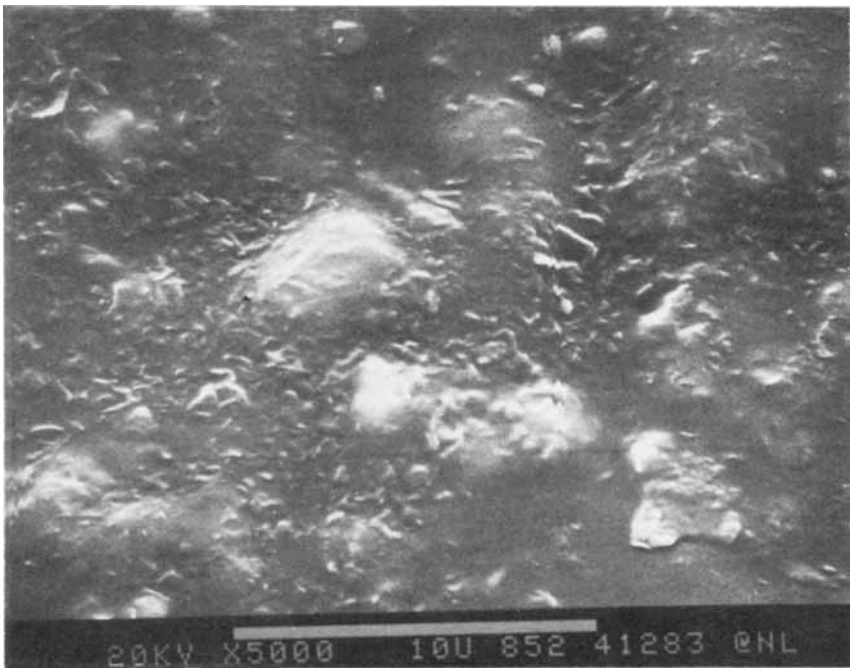

Fig. 15. Surface texture of exposed composite film with S/C 80/20 filler at higher magnification (× 2500).

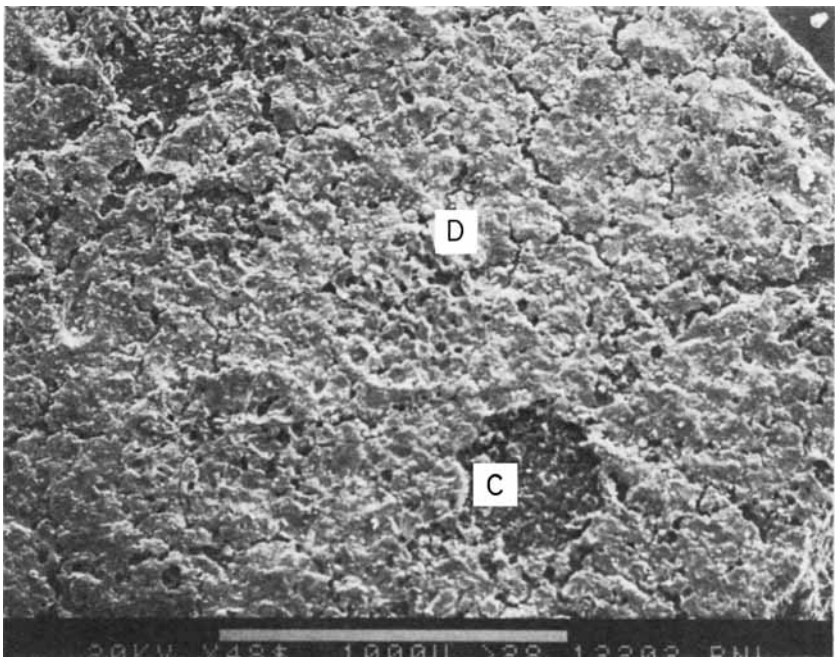

Fig. 16. Microstructure of exposed composite film with S/C 30/70 filler showing two phases.

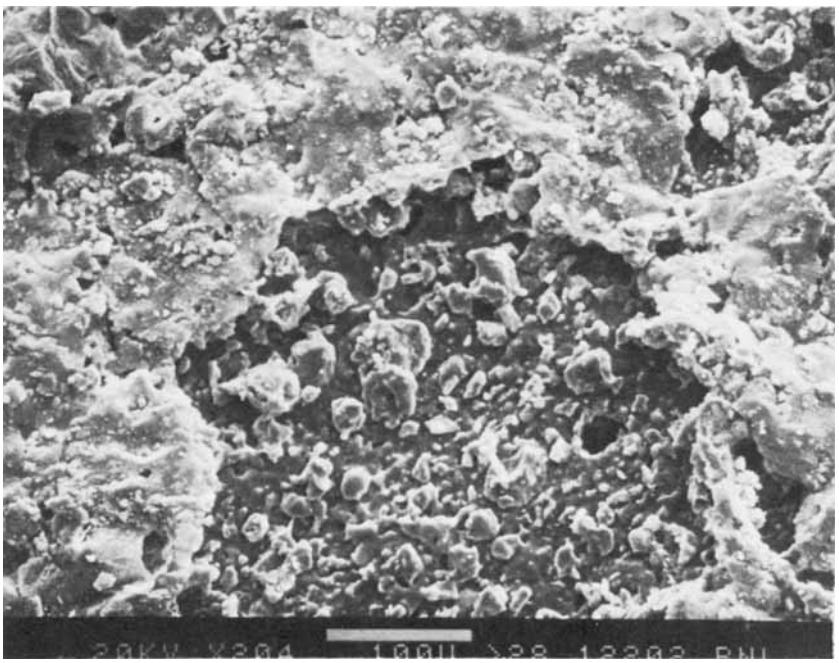

Fig. 17. Enlargement of section C in Figure 16.

To estimate the thickness of the assembled ionomer complex protective layers, the morphology at the complex/fresh layer interfaces was observed at a higher magnification (× 760, Fig. 18). Short radiating and interlocking fibers of cyrstalline hydrated cement can be seen in the protective complex layers. Since this randomly oriented hydration compound is composed of fiberlike crystals ~7 μm long, the protective layers are at least 7 μm thick. The interlocking fibers embedded in the layers may act as reinforcement for the protective complex phases.

Because identification of hydration compounds is very important in understanding the hydration process and the structure of cement, X-ray powder diffraction (XRD) studies with CuKα radiation were done. The XRD patterns in the diffraction range of 6.32–2.25 Å indicated that the phases consist of two hydrated compounds and silica (SiO_2). One of these hydration compounds is calcium silicate hydrate (C—S—H), characterized by the broad spacing at 3.03 Å, and the other is $Ca(OH)_2$ as a minor compound, represented by the weak peaks at 4.87 and 2.62 Å. The morphological features of $Ca(OH)_2$ are generally characterized as a larger lamellate hexagonal crystal.[6] Accordingly, the ternary crystalline fiber formed after exposure for 3 days to water at 150°C must be regarded as a moderately crystallized C—S—H compound formed during setting of the cement. The amount of C—S—H formations growing outward from cement grains increases with exposure time, and such growth may fill the spaces between the original cement grains and between the cement grains and the complexed ionomers. Furthermore, the orientation of closely packed gel structure may lead to the formation of interconnecting crosslinks between their surfaces, cementing the whole mass together.

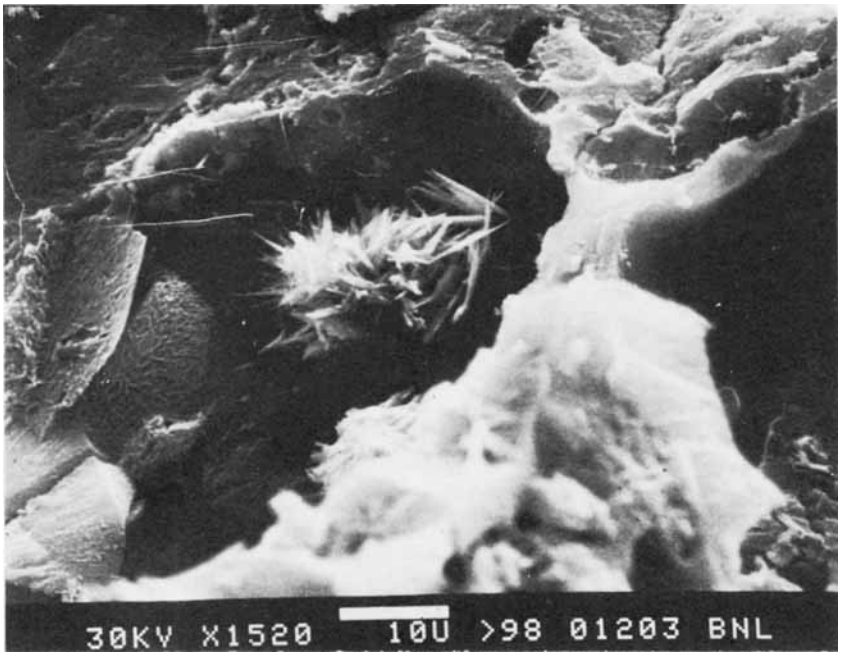

Fig. 18. Fibrous or needlelike crystals of hydrated cement produced in ionomer-complexed layers.

Properties of Films as Protective Coatings for Metals

Experiments were done to evaluate the feasibility of using inorganic macromolecular–ionomer composite films as hydrothermally stable protective coatings for metal surfaces. The objective was to investigate the intrinsic adhesion forces acting between the ionomer compounds and metal surface, the spreading behavior on wet metal surfaces, and the spreading kinetics of metal by the resin. Since surface treatments of metals can significantly improve adhesion of polymers to metallic surfaces, the use of phosphoric acid (H_3PO_4) treatments was studied. Metal plates, 50 × 15 × 2 mm, were immersed in a dilute solution of pH 4 H_3PO_4. Clean metal plates polished with ultrafine emery paper were tested for comparison.

Shear Bond Strength

The shear strength of metal-to-metal adhesive was determined by the modified ASTM Method D-1002, on specimens with an average adhesive thickness of 7 mil (see Fig. 19). After curing of deposited composite films with S/C 100/0 or 70/30 filler, the samples were exposed in an autoclave for 3 days at 150°C. Plots of lap shear bond strength vs. exposure time for chemically modified and polished samples (Fig. 19) show that surface modification greatly improves the adhesion strength in unexposed samples by about a factor of 3. When discussing lap shear strength, it should be kept in mind that the edges of the lap as stress concentration points carry a high portion of the load so that the load at which a specimen fails has a value substantially below the true strength of the adhesive. For the phos-

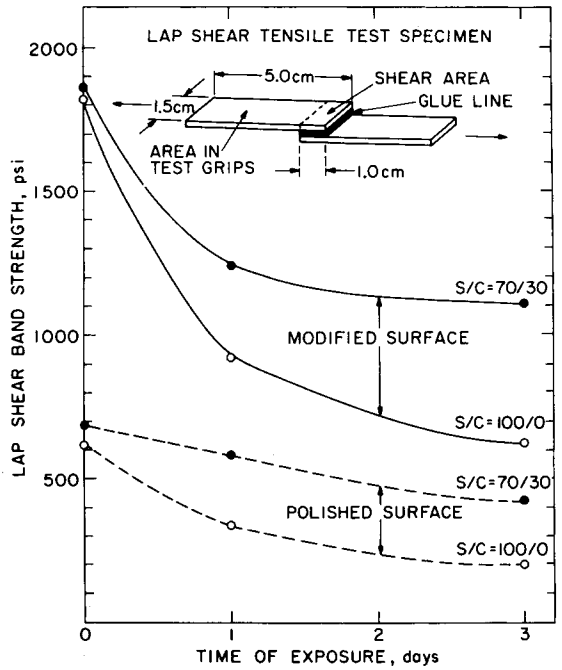

Fig. 19. Variation in ultimate shear strength with time of exposure in an autoclave at 150°C.

pated metal surfaces, the original strength of the silica-filled adhesives was almost equivalent to that of the material with S/C 70/30 filler, but their metal-to-metal bond strength decreased rapidly with increased exposure time, dropping by ~61% in 3 days to 710 psi. The adhesives with filler containing cement showed less reduction in strength. The specimens with polished surfaces showed similar trends.

These results indicate that the silica–copolymer adhesives underwent deterioration in the hydrothermal environment, leading to corrosion of the metal and lessening of the adhesion, presumably due to weakening of the interfacial layer. In the adhesives with filler-containing cement, hydrolytic deterioration of the copolymer binders occurs, but the products are converted into the ionomer conformations which connect the hydrated cement macromolecules. The newly assembled ionomer complexes have a significant function in maintaining the joint force at the adhesive–adherend interfaces. Also, the half-salt formations (—$Ca^{2+}OH^-$) on the pendent portions in the polymer molecules are thought to react with the reactive oxide surface of the metal via the flexible hydrogen bonds in the initial reaction process. As the reaction progresses, the hydrogen bond formations are converted into more rigid metal crosslinking structures (—Ca^{2+}—$^-$O—metal surface) which result in strong interfacial interaction with the oxide substrates.

Spreading Behavior of Wet Metal Surface

The moisture present on oxidized metal surfaces is an important factor affecting spreadability and the bonding forces at polymer-metal interfaces. The influence of humidity on the phosphated substrates was assessed by measuring the contact angle θ of a drop of uninitiated MMA–TMPTMA mix resin placed on the modified metal surfaces. Metal samples that had been exposed to an atmosphere of 100% relative humidity (RH) at 24°C for up to 10 days were used in this test series.

The contact angles and the adhesion tension, $\gamma_{LV} \cos \theta$, as a function of the time of exposure to 100% RH, are listed in Table III. The values of the adhesion tension,[23] which indicates the magnitude of the liquid spreadability on the solid surface, were calculated from values for the contact angles and the surface tension, γ_{LV}, of MMA–TMPTMA resin. The measured γ_{LV} of the resin at 24°C was 32.10 dyn/cm.

TABLE III
Contact Angles and Adhesion Tensions of MMA–TMPTMA Monomer on H_3PO_4-Treated Metal Surface as a Function of Time of Exposure to 100% RH

Time of exposure to 100% RH (days)	Contact angle θ (deg)	Adhesion tension $\gamma_{LV} \cos \theta$ (dyn/cm)
0	48	21.48
1	52	19.76
3	59	16.53
5	63	14.57
10	78	6.67

As expected, the contact angle, which was 48° for the unexposed metal surface, increased continuously with increased exposure time. For samples exposed for 10 days, the angle was 78°, ~63% greater than the initial value. Conversely, the adhesion tension value declined with exposure time, to a value of only 6.67 dyn/cm for samples exposed for 10 days. These results suggest that moisture on the substrate has a significant influence on the magnitude of the spreading force of resin, and that insufficient spread will lower the adhesion strength at the polymer–metal boundary.

To investigate the effects of moisture on polymer composite–metal interfacial bonding, samples for measuring the lap shear bond strength were prepared by joining moisturized metal substrates with polymer composite adhesives having S/C = 100/0 and 70/30 additive ratios. The surfaces of all metal substrates used in these tests were treated with H_3PO_4 solutions. The test results (Fig. 20) indicate that plotting the fraction on initial lap shear bond strength against time of exposure to 100% RH gives a straight line. A more interesting observation is that the bond strength of cement-containing adhesives decreases less with exposure time than does that of silica–copolymer adhesives, being >90% of the originial value for the former and 67% for the latter, for samples exposed for 10 days.

The above findings can be interpreted by the following hypothetical mechanisms of reaction between the composite adhesives and the moisturized metal surfaces. When the oxidized metal surface is exposed in a high humidity environment, the electronegative oxygen atoms on the phosphated layers become polarizable and susceptible to the formation of coordinate and hydrogen bonds with H_2O molecules. Once the hydration of the oxidation phase occurs, the newly formed layers are characterized by the ability to decrease the adhesion tension energy of resins.[29] Consequently, the bond-

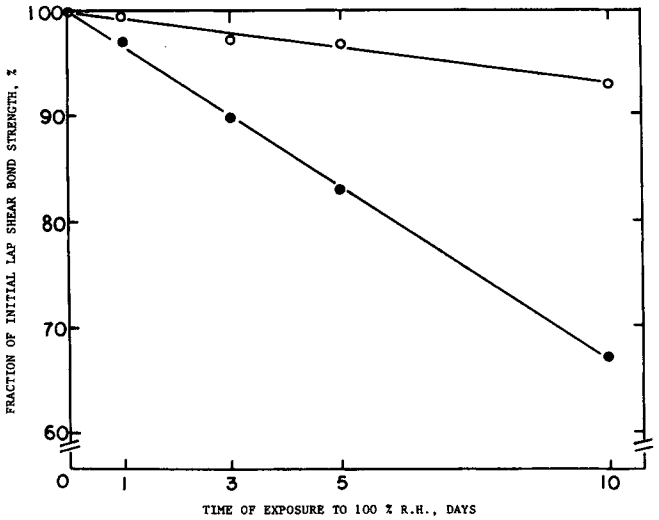

Fig. 20. Bond strength reduction of phosphate-treated metal as a function of time of exposure to humidity: (○) copolymer adhesive with S/C 30/70 filler; (●) adhesive with S/C 100/0 filler.

ing forces of silica–copolymer adhesive are thought to depend mainly on the degree of hydration of the phosphate metal surfaces. On the other hand, when the organic adhesive with cement-containing filler, having an abundant supply of Ca^{2+} ions, is in contact with wet surfaces, the cement grains, as divalent metallic ion donors, are acted upon by moisture to produce Ca^{2+} ions. The Ca^{2+} ions liberated from the cement react rapidly with H_2O molecules to yield coordination compounds having a complex conformation with up to six molecules of water in the form of an octahedral structure. The introduction of Ca^{2+} ions into the decomposable hydration phosphate compounds will break—0^-—$^+$H—O—H bonds. Subsequently, Ca^{2+} ions coordinated with neutral H_2O molecules may electrically connect the phosphated layers and the polymer molecules. This cohesion force of divalent metallic ions may lead to the enhancement of the adhesion forces at the polymer-hydrated metal interface.

Spreading Kinetics of Dry Metal Surface by Resin

Although the magnitude of the spreading force of the substrate by resin depends on the polarizability, heterogeneity, and the topography of the solid surface, the change in the initial contact angle as a function of time varies with temperature. It was of interest to consider the implication of a time-dependent contact angle on modified metal surfaces, and experiments were done in which the advancing contact angle of resins was followed, to determine factors that could reliably define the kinetics of spreading.

The advancing contact angles of MMA–TMPTMA mix resin on the phosphate-treated metal substrates were measured at temperatures >40°C, at which the spread at the boundary of a discrete resin droplet takes a relatively long time, ~20 min. Initial information regarding the spreading kinetics was obtained by using Newman's[30] relation, derived from the dynamic theory of classical capillary flow:

$$\ln\left(1 - \frac{\cos \theta_t}{\cos \theta_\infty}\right) = \ln a - Ct$$

where θ_t is the contact angle at time t, θ_∞ is the contact angle at infinite time, a is a constant, and C is the spreading coefficient. The factor $(1 - \cos \theta_t/\cos \theta_\infty)$ is defined as the rate of advance of the contact angle of the liquid adhesive. A plot in the $\ln(1 - \cos \theta_t/\cos \theta_\infty)$ against t should give a straight line intersecting the ordinate (where $t = 0$) at $\ln(1 - \cos \theta_t/\cos \theta_\infty) = \ln a$ and having a slope of a $\Delta \ln(1 - \cos \theta_t/\cos \theta_\infty)$ vs. Δt plot. The spreading coefficient C can be calculated from the slope.

Plots of advance in contact angle at 40°, 50°, 60°, and 70°C (Fig. 21) show that the rate of advance is a linear function of time. The required values of the spreading coefficient C obtained from the slopes of the lines are listed in Table IV. They tend to increase with increasing temperature. This apparently verifies that the boundary of a sessile drop is significantly advanced by elevated temperature; the value of 2.71×10^{-3} s^{-1} at 70°C was ~2.2 times that at 40°C.

These results indicate that the increased coefficient value corresponds to a higher rate of spreading of the substrate by the adhesives, which enhances

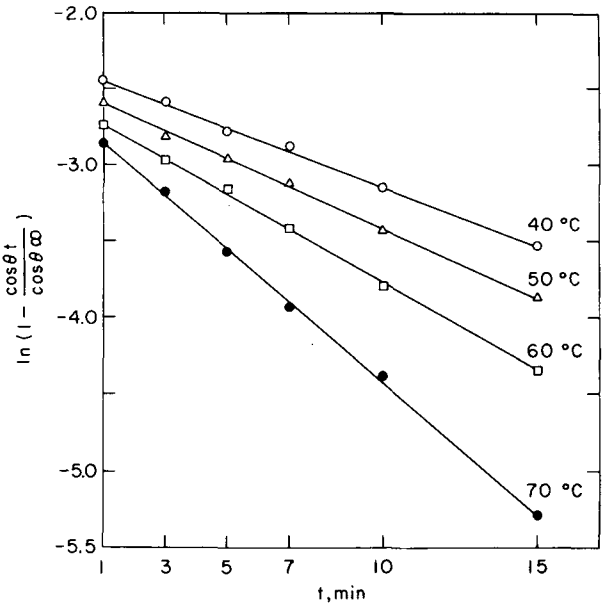

Fig. 21. Rate of advance of contact angle of MMA–TMPTMA resin on modified metal surfaces at various temperatures.

the joint strength at the metal–adhesive interface. This work reconfirmed that the spreading coefficient is an important parameter for determining the degree of affinity between the adhesive and the modified substrate surface.[31,32]

When the topographical aspects of modified metal surfaces are studied, it is generally accepted that good wettability between the adhesives and porous oxide layers relates directly to the penetration of resin into the capillary pores on oxidized metal surfaces. The approximate penetration depth into a capillary of a resin having a known viscosity can be predicted by means of Packham's[33] expression, which was derived from modification of the Washburn and Newman equations.[34] The modified equation is given as follows:

$$X_t^2 = \frac{r\gamma_{LV}\cos\theta_\infty}{2\eta}\left(t - \frac{a}{c} + \frac{ae^{-Ct}}{c}\right)$$

TABLE IV
Spreading Coefficient C of MMA–TMPTMA Resin on Phosphated Layers at Various Temperatures

Temp (°C)	Spreading coefficient C (s^{-1})
40	1.21×10^{-3}
50	1.40×10^{-3}
60	1.79×10^{-3}
70	2.71×10^{-3}

where X_t is the penetration depth at a given time t, r refers to the radius of the pores, η is the viscosity of the resin, γ_{LV} refers to the surface tension of the resin, $\cos \theta_\infty$ is the contact angle at infinite time, and a and C are the constant parameters obtained from Newman's equation.

To obtain information regarding the distance penetrated by the MMA–TMPTMA blend resin, an experiment was performed at ambient temperatures of 40°C and 60°C and a penetration time of 15 min. The surface tension and viscosity measured for the resin at each temperature are presented in Table V. These data were used to calculate the depth of penetration in pores of a radius ranging between 100 μm and 100 Å, and the results are given in Table V. The data indicate that the predicted penetration depth is primarily dependent upon the surface tension and viscosity characteristics of the resin. It appears that resins having low surface tension and viscosity values are able to fully fill pores with a radius in the order of an angstrom unit that exist in typical oxidation layers, thereby enhancing the bonding strength at the adhesive–oxidized substrate interfaces.

CONCLUSIONS

In studying the physicochemical factors affecting the hydrothermal stability of hydrated inorganic macromolecule–ionomer composite materials for utilization as protective coatings on metals, the following generalizations can be conclusively drawn from the results described above. In the formation of the ionomer, the quantity of $COO^-(Ca^{2+})$ groups produced by ionic reactions occurring between the carboxylate anions and the nucleophilic Ca^{2+} ions during exposure to hot water increases with increasing hydrothermal temperatures and higher concentrations of the cement used as a source of divalent metallic cations. Evidently, the conformation of a Ca salt bridge not only acts to inhibit the scission of the polymer chains due to hydrolysis of the pendent groups, but also contributes significantly to the thermal stability of ionomer matrices near 300°C. This was indicated by TGA and DTA evaluations. These data also revealed that the small amount of $Ca(OH)_2$ formations on the ionomer layers is produced as one of the hybrid hydration

TABLE V
Predicted Penetration Rate in 15 min of an MMA–TMPTMA Resin at 40°C and 60°C as a Function of Open Pore Radius Size

Ambient temp (°C)	Resin		Radius of capillary pore	Penetration depth (mm)
	Surface tension, (dyn/cm)	Viscosity (cP)		
40	31.3	203	100 μm	2.311
40	31.3	203	10 μm	0.731
40	31.3	203	1 μm	0.231
40	31.3	203	1000 Å	0.073
40	31.3	203	100 Å	0.023
60	30.0	120	100 μm	2.978
60	30.0	120	10 μm	0.942
60	30.0	120	1 μm	0.298
60	30.0	120	1000 Å	0.094
60	30.0	120	100 Å	0.030

macromolecules of cement. SEM examination of the morphology indicated that the ionomer composites combined with the hybrid macromolecules to form very thin superficial layers on the films. The superficially formed C—S—H macromolecule–ionomer layers are at least ~7 μm thick and act to prevent severe deterioration of the composite films due to hydrothermal agglomeration of the copolymer matrices. The major hydration macromolecules of cement formed during the 3-day exposure in the autoclave at 150°C were identified to be the C—S—H compounds moderately crystallized on the outward cement grains. These are primarily responsible for the mechanical enhancement since they act as a reinforcement for the protective ionomer layers.

Once these components become the constituents of a film, the film acquires some very interesting characteristics. One of inherent properties is that the glass transition temperature T_g, tends to increase with increasing cement concentration. This affects the chain stiffness of the polymer molecules. A maximum T_g of 63.5°C was attained when 50 parts silica flour and 50 parts cement were used, and the addition of more cement decreased the T_g. Trends similar to those for the T_g were seen in the measurements of tensile strength of the films.

Analysis of the above data indicates that interactions at the interface between the configurated hydration macromolecules and the ionomer chains not only result in strong agglomeration and chain entanglement, but also are likely to contribute to incremental interfacial stresses which lead to chain enlargement occurring along with the growth of macromolecules.

Another characteristic observed is that the Ca-complexed ionomer films have a lower water permeability than the exposed films having silica flour filled without cement. A possible reason for this is as follows: The copolymer films with silica flour–filler, after exposure to hot water, contain a larger number of hydrophilic carboxylate groups yielded by water hydrolysis of the functional carboxyl groups in the polymer molecule. Contact angle measurements indicated a high surface-free energy $\gamma_S > 50$ erg/cm^2, and a water wettability >100 erg/cm^2. In contrast, the complex ionomer films containing the Ca salt formation coordinated with 6 H_2O ligands are more hydrophobic. Thus, the total surface free energy for the films with S/C 70/30 filler after exposure to water at 150°C, was calculated to be ~34 erg/cm^2, ~42% lower than that for films with S/C 100/0 filler. Conversely, the production of excessive cement macromolecules results in an increase in surface energy. This is connected with changes in surface roughness due to the squeezing deformation of the film. The results suggest that the low water permeability of the exposed films is directly related to lower hydrophilicity, low-energy surface, and reduced surface roughness.

The high bonding force between the cement–copolymer material and the phosphate-treated metal surfaces is the third important characteristic. Even when the chemically modified metal surface is completely wet, the metal-to-metal lap bonding strength decreased $<10\%$. The reason for this excellent bonding to the wet surfaces is thought to be that the Ca^{2+} ions dissociated from the cement grains in contact with moisture break the decomposable hydration phosphate compound formed on the metal surfaces,

and, subsequently, Ca^{2+} ions electrically connect the phosphated layers and the polymer molecules. Furthermore, the ionomer complex adhesive produced during exposure in the hydrothermal environment maintained the joint strength at the adhesive–adherend interface. This was thought to be due to the strong crosslinking action of Ca^{2+} metallic ions connecting the reactive oxide substrates and the ionomer molecules. The high spreadability of metal surfaces by the liquid adhesives is one of the important factors affecting the good bonding characteristics. In seeking to elucidate the degree of spreading at different temperatures, it was reconfirmed that the spreading coefficient obtained from Newman's equation is an important parameter in fully understanding the kinetics of spreading.

References

1. T. Sugama, L. E. Kukacka, and W. Horn, *J. Appl. Polym. Sci.*, **24**, 2121 (1979).
2. T. Sugama, L. E. Kukacka, and W. Horn, *J. Mater. Sci.*, **15**, 1498 (1980).
3. T. Sugama, L. E. Kukacka, and W. Horn, *J. Mater. Sci.*, **16**, 345 (1980).
4. Kh. S. Mamedon and N. V. Belov, *Dokl. Akad. Nauk SSSR*, **140**, 615 (1956).
5. I. Souma, *J. Appl. Polym. Sci.*, **27**, 1523 (1982).
6. T. Sugama and L. E. Kukacka, *Cem. Concr. Res.*, **12**, 789 (1982).
7. P. M. Parker, C. Clement, and R. M. Beirute, *Oil Gas J.*, **21**, 9 (1977).
8. Yu. S. Lipaton, *Dokl. Akad. Nauk SSSR*, **143**, 1142 (1962).
9. I. Galperin, *J. Appl. Polym. Sci.*, **11**, 1475 (1967).
10. G. J. Howard and R. A. Shanks, *J. Appl. Polym. Sci.*, **26**, 3099 (1981).
11. D. H. Droste and A. T. Dibenedetto, *J. Appl. Polym. Sci.*, **13**, 2149 (1969).
12. K. Iisaka and K. Shibayama, *J. Appl. Polym. Sci.*, **22**, 3135 (1978).
13. L. E. Nielsen, *J. Appl. Polym. Sci.*, **17**, 1897 (1979).
14. L. B. Clapp, *The Chemistry of the OH Group*, Prentice-Hall, Englewood Cliffs, N.J., 1967, p. 24.
15. A. D. Wilson and S. Crisp, *Br. Polym. J.*, **7**, 279 (1975).
16. J. E. Field and L. E. Nielsen, *J. Appl. Polym. Sci.*, **12**, 1041 (1963).
17. L. D. Wakeley, B. E. Scheetz, M. W. Grutzeck, and D. M. Roy, *Cem. Concr. Res.*, **11**, 131 (1981).
18. F. M. Lea and C. H. Desch, *The Chemistry of Cement and Concrete*, Edward Arnold, London, 1956, p. 225.
19. L. H. Lee, *J. Appl. Polym. Sci.*, **12**, 719 (1968).
20. T. Young, *Phil. Trans. Roy. Soc. (London)*, **95**, 65 (1805).
21. A. Dupre, *Théorie mechanique de la chaleur*, Gouthier-Villars, Paris, 1869, p. 369.
22. W. A. Zieman, *Ind. Eng. Chem.*, **55**, 18 (1963).
23. H. W. Fox and W. A. Zisman, *J. Colloid Sci.*, **5**, 514 (1950).
24. D. K. Owens and R. c. Wendt, *J. Appl. Polym. Sci.*, **13**, 1744 (1969).
25. A. Baszkin and L. Ter-Minassian-Saraga, *J. Colloid Interface Sci.*, **43**, 190 (1973).
26. F. M. Fowkes, *J. Phys. Chem.*, **66**, 1863 (1962).
27. E. Baer, *Engineering Design for Plastics*, Reinhold, New York, 1964, p. 690.
28. F. M. Fowkes, *Chemistry and Physics of Interfaces*, American Chemical Society, Washington, D.C., 1965, Chap. 1, p. 8.
29. K. W. Allen, *Adhesion 1*, Applied Science, London, 1977, p. 269.
30. S. Newman, *J. Colloid Interface Sci.*, **26**, 209 (1968).
31. B. W. Cherry and C. M. Holmes, *J. Colloid Interface Sci.*, **29**, 1974 (1969).
32. B. W. Cherry and S. El Muddaris, *J. Adhesion*, **2**, 42 (1970).
33. D. E. Packham, *Adhesion Aspects of Polymeric Coatings*, K. L. Mettal, Ed., Plenum, New York, 1983, p. 19.
34. E. D. Washburn, *Phys. Rev.*, **17**, 374 (1921).

Received October 10, 1983
Accepted January 23, 1984